The Epoxyeicosatrienoic Acid Pathway Enhances Hepatic Insulin Signaling and is Repressed in Insulin-Resistant Mouse Liver*[S]

Alexander Schäfer‡§, Susanne Neschen§¶, Melanie Kahle§¶, Hakan Sarioglu‡§, Tobias Gaisbauer§¶, Axel Imhof‖, Jerzy Adamski§¶, Stefanie M. Hauck‡§ §§, and Marius Ueffing‡§‡‡**

Although it is widely accepted that ectopic lipid accumulation in the liver is associated with hepatic insulin resistance, the underlying molecular mechanisms have not been well characterized.

Here we employed time resolved quantitative proteomic profiling of mice fed a high fat diet to determine which pathways were affected during the transition of the liver to an insulin-resistant state. We identified several metabolic pathways underlying altered protein expression. In order to test the functional impact of a critical subset of these alterations, we focused on the epoxyeicosatrienoic acid (EET) eicosanoid pathway, whose deregulation coincided with the onset of hepatic insulin resistance. These results suggested that EETs may be positive modulators of hepatic insulin signaling. Analyzing EET activity in primary hepatocytes, we found that EETs enhance insulin signaling on the level of Akt. In contrast, EETs did not influence insulin receptor or insulin receptor substrate-1 phosphorylation. This effect was mediated through the eicosanoids, as overexpression of the deregulated enzymes in absence of arachidonic acid had no impact on insulin signaling. The stimulation of insulin signaling by EETs and depression of the pathway in insulin resistant liver suggest a likely role in hepatic insulin resistance. Our findings support therapeutic potential for inhibiting EET degradation. ***Molecular & Cellular Proteomics 14: 10.1074/mcp.M115.049064, 2764–2774, 2015.***

Hepatosteatosis has a strong association with hepatic insulin resistance, which plays a major role in the early stages of type 2 diabetes. Although the contribution of the liver to total energy consumption is not as high as other tissues, the liver is the main organ responsible for endogenous glucose production through gluconeogenesis and glycogenolysis (1). The liver's pivotal role in type 2 diabetes is underscored by a strong correlation between fasting hyperglycemia and endogenous glucose production in patients (2). Studies on the early stages of hepatosteatosis and hepatic insulin resistance are complicated by the fact that patients are often unaware of their impaired insulin sensitivity. Therefore, the transition of the liver to an insulin resistant state is not as well studied as other aspects of the disease.

To study early stage hepatic insulin resistance in an unbiased fashion, we analyzed the transition of the liver to an insulin-resistant state in a mouse model fed a high fat diet (HFD)[1], rich in safflower oil, on the proteome level. Phenotypic characterization in combination with proteomic profiling resulted in the identification of alterations in protein patterns, which were correlated with hepatic insulin resistance in a time-resolved manner. Protein expression was monitored using state of the art LC-MS/MS based proteomics, employing non-targeted discovery as well as targeted strategies.

The comparison of expression profiles from HFD-fed mice with standard diet-fed controls directed us to a group of eicosanoid lipid mediators - epoxyeicosatrienoic acids (EET). Our proteomic approach uncovered a down-regulation of the

From the ‡Research Unit Protein Science, Helmholtz Zentrum München, German Research Center for Environmental Health (GmbH), Germany, Ingolstädter Landstr.1 8674 Neuherberg; §German Center for Diabetes Research (DZD), Neuherberg, Germany; ¶Institute of Experimental Genetics, Helmholtz Zentrum München, German Research Center for Environmental Health (GmbH), Germany, Ingolstädter Landstr.1 8674 Neuherberg; ‖Munich Center of Integrated Protein Science, Adolf-Butenandt Institute, Ludwig Maximilians University of Munich, Germany, Schillerstraβe 44, 80336 Munich; **Institute of Experimental Genetics, Technical University Munich, Freising-Weihenstephan, Germany; ‡‡Centre of Ophthalmology, Institute for Ophthalmic Research, University of Tübingen, Germany, Röntgenweg 11,72076 Tübingen

Received February 11,2015, and in revised form, June 7, 2015

Published, MCP Papers in Press, June 12, 2015, DOI 10.1074/mcp.M115.049064

Author contributions: A.S., S.N., H.S., S.M.H., and M.U. designed research; A.S., S.N., and M.K. performed research; T.G. and J.A. contributed new reagents or analytic tools; A.S. wrote the paper; A.I., J.A., S.M.H., and M.U. provided critical discussion and edited the paper.

[1] The abbreviations used are: HFD, High fat diet; CYP, Cytochrome P450; DHET, Dihydroxyeicosatrienoic acid; EET, Epoxyeicosatrienoic acid; FDR, False discovery rate; IR, Insulin receptor; IRS-1, Insulin receptor substrate 1; LFD, Low fat diet; MS/MS, Tandem mass spectrometry; PPAR, Peroxisome proliferator-activated receptor; SRM, Selected reaction monitoring.

EET pathway at the protein level through HFD feeding in insulin resistant mouse liver. In order to link expression patterns to signaling alterations and connect alterations on the level of signaling pathways to insulin sensitivity we proceeded to investigate the influence of these eicosanoids on insulin signaling in primary hepatocytes. Up to now, EETs have been extensively studied in the biology of blood vessels (3) and have been found to have profound influence on intracellular signaling (4–6) and ion channel activity (7) in endothelial as well as smooth muscle cell. Their vasodilating (7), anti-inflammatory (8) and proliferation inducing effects on endothelial cells (5, 6) have made inhibition of the EET degrading enzyme Ephx2 an attractive pharmacological strategy for the treatment of hypertension, with clinical trials already in progress (9).

Recent studies using genetic mouse models have shown that knockdown or overexpression of EET pathway enzymes affect insulin secretion (10) and glucose homeostasis (11, 12) and point to as yet poorly understood effects of EETs on insulin sensitivity (10, 11). Moreover, EETs have been implicated in activating insulin signaling directly by increasing insulin receptor (IR) phosphorylation (11). In line with this model, medium supplementation, but not acute stimulation of the human hepatoma cell line HepG2 with high doses (30 μM) of EETs, has been shown to increase insulin mediated activation of Akt, the central protein kinase in insulin signaling (13).

We show here that acute application of 4 μM of exogenous EETs but not overexpression of the EET pathway enzymes in absence of arachidonic acid had a strong positive effect on insulin mediated phosphorylation of Akt in primary mouse hepatocytes. The activation was not associated with changes in IR or insulin receptor substrate-1 (IRS-1) tyrosine phosphorylation through EETs. These results indicate that EET influence insulin signaling downstream of IRS-1 and upstream of Akt rather than at the level of the IR.

EXPERIMENTAL PROCEDURES

Mice—C3HeB/FeJ mice were maintained on low fat chow diet (LFD) (13% fat-derived calories, 4 kcal/g, Diet#1310, Altromin, Germany). At 14 weeks of age, male mice were matched for body mass and litter and single-housed. Four groups of mice were then given free access to a HFD (58% fat-derived calories, 6 kcal/g, Ssniff, Germany) for 2, 7, 14, or 21 days. The majority of fatty acids in the HFD were linoleic acid (C18:2, ω-6). Initial body mass-, age-, and litter-matched control groups were continued on chow diet. At the end of the study, random-fed mice were killed with isoflurane. The liver was freeze-clamped and stored at −80 °C. All animals received humane care according to criteria outlined in the NAS 'Guide for the Care and Use of Laboratory Animals'. All animal experiments were approved by the Upper-Bavarian district government (Regierung von Oberbayern Gz.55.2-1-54-2532-4-11).

Liver Membrane Protein Extraction and Tryptic Digestion—Membrane proteins were enriched as described previously (14) with the following modifications: Liver samples were homogenized in high-salt buffer (2 M NaCl, 1 mM EDTA, 10 mM HEPES pH 7.4) using a Precellys 24 Homogenizer (Peqlab, Erlangen, Germany) pre-chilled to 0 °C. Homogenates were cleared by centrifugation at 10.000g for 30 min at 4 °C. Membrane vesicles were harvested at 100.000g at 4 °C for 30 min. The next steps were carried out as described in (14). Resulting protein pellets were resuspended in 50 mM Tris pH 8.5 0.5% (w/v) Rapigest (Waters, Eschborn, Germany). Proteins were reduced and alkylated using 7 mM dithiothreitol at 60 °C for 10 min followed by 22 mM iodoacetamide for 30 min at room temperature. Proteins were digested with 5 μg trypsin for 18h at 37 °C. Afterward Rapigest was hydrolyzed by lowering the pH below 2 on ice for 30 min.

LC-MS/MS Based Proteomics and Label-Free Quantification—Quantitative non-targeted proteomics data were generated with an LC-MS system composed of an Ultimate 3000 nano HPLC (Dionex, Idstein, Germany) coupled to an Orbitrap XL mass spectrometer (Thermo Fisher, Bremen, Germany), equipped with a nano-ESI source. ESI was maintained with a spray voltage between 1.25–1.4 kV without sheath or auxiliary gas flow and transfer capillaries heated to 200 °C.

Peptides were loaded onto a nano trap column (0.3 × 5 mm, PepMap100 C18, 5 μm, 100 Å; LC Packings) in 0.1% (v/v) TFA at a flow rate of 30 μl/min for 5 min and separated on a PepMap column (0.075 × 150 mm, 3 μm, 100A° pore size (Dionex)) with a nonlinear 170 min gradient using 2% (v/v) acetonitrile, 0.1% formic acid (v/v) in water (A) and 0.1% (v/v) formic acid in 98% (v/v) acetonitrile (B) at a flow rate of 300 nl/min with the gradient settings: 0–140 min: 5–31% B. 140–145 min: 31–99% B. 145–150 min: 99% B and equilibrate for 10 min at starting conditions.

Survey full scan MS spectra (from m/z 300 to 1500) were acquired in the Orbitrap with resolution r = 60,000 at m/z 400. Continuous internal calibration with polysiloxane (m/z = 445.12002) as lock mass was used. The method allowed sequential isolation of up to ten precursors depending on signal intensity, for fragmentation in the linear ion trap using CID with an AGC target value of 10.000, normalized collision energy set to 35% and an activation time of 30 ms. Minimum signal intensity required was 200 and isolation width was 2 amu. Precursor masses were selected in a data-dependent manner. High resolution MS scans in the orbitrap and MS/MS scans in the linear ion trap were performed in parallel. Target peptides already selected for MS/MS were dynamically excluded for 30 s.

Label-free quantification was performed using Progenesis QI for proteomics 2.0 (Non-Linear Dynamics, Newcastle, UK). Runs were aligned semi-automatically and peak picking performed with default settings. MS/MS spectra were searched against the Ensembl Mouse database (Release 72, 06/2013, 51765 sequences) using Mascot 2.5.0 (Matrix Science, London, UK) with the parameters: Precursor mass tolerance: 7 ppm, fragment tolerance: 0.7 Da, enzyme: trypsin, missed cleavages: 1, instrument: ESI-TRAP, fixed modifications: carbamidomethylation (C), variable modifications: acetylation (K), oxidation (M) and deamidation (N, Q). Search results were further processed using Percolator (15). Posterior error probability was adjusted to ≤1% by using a Percolator cutoff of 20, yielding peptide FDR values of ≤1% as confirmed by decoy database searches. Peptides were excluded from quantification if they were not unique or contained methionine and two unique peptides were required for each protein. Protein FDR was estimated by decoy database search and found to be lower than 0.5% for all datasets. Proteins were grouped in Progenesis QI 2.0 by identifying lead proteins and subsuming proteins identified only by a subset of a lead protein's peptides in the respective protein group. The resulting protein groups and peptides are provided in Supplement Table I and Supplement Table II, respectively. Quantification was based on XICs of unique peptides without intensity thresholds. The normalization implemented in Progenesis QI 2.0 was applied to all peptide abundances. Peptide MS abundances were combined into protein MS intensities using Progenesis QI 2.0 default settings. Mean, S.D. and average fold changes for each protein, based on the proteins MS intensities, are provided in Supple-

ment Table I. *p* values based on one-way ANOVA were calculated by Progenesis QI 2.0 and corrected for multiple testing using the Benjamini Hochberg method.

LC-SRM and Absolute Quantification—Absolute amounts of EET epoxygenases and Ephx2 normalized to $\beta\gamma$-actin were determined by LC-SRM. Recombinant His-tagged [$^{13}C_6{}^{15}N_4$]-L-arginine and [$^{13}C_6{}^{15}N_2$]-L-lysine labeled proteins were expressed in *E. coli* using pDEST-17 subcloned EET enzymes and purified as described for the QconCAT in (16). Recombinant proteins were digested in solution as described above and quantified by LC-SRM using the light AQUA peptide STSLYK; a sequence tag, which was present in the His-tag linker region of all recombinant proteins. Heavy standard peptides were stored at −80 °C and used to set up SRM assays for all four proteins according to established criteria (17). Standard peptides for $\beta\gamma$-actin were derived from the QconCAT described in (16). All proteotypic peptides and SRM parameters for the assays are provided in Supplement Table III. Crude protein extracts from liver were generated and digested as described in (16) and heavy labeled standard peptides were added. LC-SRM/MS analysis was performed on a Tempo nano MDLC system coupled online to a Q-Trap 4000 (AB Sciex) mass spectrometer by a nano spray III ion source. Peptides were loaded onto a nano trap column (0.3 × 5 mm, PepMap100 C18, 5 μm, 100 Å; LC Packings) in 0.1% TFA at a flow rate of 20 μl/min for 5 min and separated on a C18 analytical column (0.075 × 150 mm, PepMap100 C18, 3 μm, 100 Å, LC Packings) using a 60 min gradient of 2% acetonitrile, 0.1% formic acid in water (A) and 0.1% formic acid in 98% acetonitrile (B) at a flow rate of 250 nl/min. The gradient settings were: 5–35 min: 5–45% B, 35–40 min: 45–90% B, 40–42 min: 90% B, 42–49 min: 90–5% B, re-equilibration for 10 min. Electrospray ionization was maintained with curtain gas set to 14 psi, a spray voltage of 2.6 kV, ion source gas set to 30 psi and an interface heater temperature of 170 °C. Peptide measurements were conducted with Q1 and Q3 set to unit resolution using scheduled SRM with a retention time window of 3 min and a target scan time of 5s. Absolute protein amounts were determined using MultiQuant 1.2 (AB Sciex). Significant differences were determined using Student's *t* test.

Insulin Stimulation of Primary Hepatocytes and Cell Lines—Primary hepatocytes were isolated by collagenase/EGTA perfusion as published elsewhere (18) from male C3HeB/FeJ mice. Following preparation, hepatocytes were resuspended in Williams E Medium (Gibco, Paisley, UK, Catalogue Number 32551), 10% (v/v) FCS, 100 nM dexamethasone. The hepatocyte cell lines Hepa 1–6 and BNL CL.2 were obtained from ATCC (Manassas, VA) and cultured in DMEM (Gibco, Catalogue Number 41966), 10% (v/v) FCS.

For stimulation experiments, cells were seeded onto collagen I coated six-well plates and cultured in serum-free starvation medium (Williams E medium and DMEM for primary hepatocytes and hepatocyte cell lines, respectively). Subsequently, cells were pre-treated with EETs (4 μM of 5(6)-EET, 8(9)-EET, 11(12)-EET and 14(15)-EET (Cayman Chemicals, Ann Arbor, MI) or vehicle (DMSO) in starvation medium for 1h at 37 °C 5% CO_2. Next, cells were stimulated with starvation medium containing the indicated concentrations of human insulin (Sigma-Aldrich, Steinheim, Germany) with or without EETs at the same concentration as above. Stimulation media for this second step were supplemented with Phosphatase Inhibitor Mixture 2 and 3, (Sigma-Aldrich) at 1:200. DMSO was added to wells without EETs to yield the same final concentration in all wells of the experiment. Cells were incubated for 20, 40 or 60 min at 37 °C 5% CO_2 and scraped into 50 μl RIPA buffer.

Western Blot—Ten μg total protein were separated by SDS-PAGE and wet-blotted onto polyvinylidene fluoride membranes. Membranes were blocked in TBS-T 5% (w/v) skim milk for 1h at room temperature and incubated with primary antibodies diluted in TBS-T 5% (w/v) BSA overnight at 4 °C. The following primary antibodies were used: Cell Signaling Technology (Leiden, The Netherlands): Akt, IRS-1 and phospho-Akt (S473); Santa Cruz Biotechnologies (Santa Cruz, CA): Ephx2; Millipore (Billerica, MA): phospho-IR (Y1179/80), GAPDH and phospho-IRS-1 (Y608); Sigma-Aldrich: β-Actin and Flag-M2. Membranes were washed thrice in TBS-T incubated with horseradish peroxidase couple secondary antibodies (Jackson ImmunoResearch, Westgrove, PA) diluted 1:7500 in TBS-T 5% (w/v) BSA for 1h at room temperature. After washing the membranes four times in TBS-T, they were immersed in enhanced chemoluminescent solution. Chemoluminescence was recorded with a digital developer. Bands were quantified using Image Studio Lite 4.0 (LI-COR, Lincoln, NE).

Cloning and Transfection of EET Enzymes—Total RNA from C3HeB/FeJ mouse liver was extracted as described in (19) and converted into cDNA using the RevertAid First Strand cDNA Synthesis Kit (Thermo Scientific, Waltham, MD) according to the manufacturer's instructions. EET enzymes were cloned into the expression vectors pcDNA3/DEST, pDEST17 (N-terminal His tag) (Invitrogen, Carlsbad, CA) and pDEST-N-SF-TAP (20) using the Gateway cloning system according the manufacturer's instructions.

Hepa 1–6 were transfected with 3 μg plasmid DNA using Lipofektamine 2000 (Invitrogen), according to the manufacturer's instructions. Transfected Hepa 1–6 cells were subjected to insulin stimulation as described above.

Eicosanoid Analysis of Hepa 1–6 Cell Lysates—Hepa 1–6 cells were scraped into reducing lysis buffer (50 mM Tris, 10% (v/v) methanol, 1 mM TCEP, 0.1% SDS, pH 8). Lipids were prepared by methanol-chloroform precipitation, dried completely by vacuum centrifugation and reconstituted in 50 μl 65% acetonitrile. Eicosanoids were separated on a Prominence HPLC (Shimadzu, Kyoto, Japan) equipped with a C18 analytical column (2.1 × 250 mm, Hypersil C18, 5 μm, 130 Å; Thermo Scientific) using a binary multistep gradient with eluents A (H_2O, 0.1% (v/v) formic acid) and B (acetonitrile, 0.1% (v/v) formic acid). Eicosanoids were detected by a Q-Trap 4000 mass spectrometer (AB Sciex) operated in negative ion SRM mode.

Pathway Enrichment Analysis—Cohorts of mice (n = 6–8) were compared by non-targeted label-free proteomics for each time point. Enriched KEGG and Reactome pathways were determined based on regulated proteins using the online tool DAVID (21). *p* values calculated by DAVID were corrected for multiple testing (Benjamini Hochberg, FDR< 5%).

RESULTS

HFD Induced Hepatic Insulin Resistance is Associated with Proteome Changes—We studied the impact of safflower oil HFD feeding on protein expression patterns by label-free quantitative proteomic profiling in a recently published model of hepatosteatosis and hepatic insulin resistance (22). HFD feeding induced hepatosteatosis after 2 days. While HFD-fed animals remained normoglycemic, they developed modest hyperinsulinemia compared with LFD-fed littermates. Insulin action on the whole body and organ level for this model has previously been determined using the euglycemic-hyperinsulinemic clamp technique. HFD markedly impaired whole body insulin sensitivity after 14 and 21 days compared with LFD controls (22). Concurrent with whole body insulin resistance, mice developed hepatic insulin resistance after 14 and 21 days (22).

Due to limited analytical depth, current proteomic techniques cannot cover the whole proteome of a mammalian organ. Focusing on membrane bound components at the cost

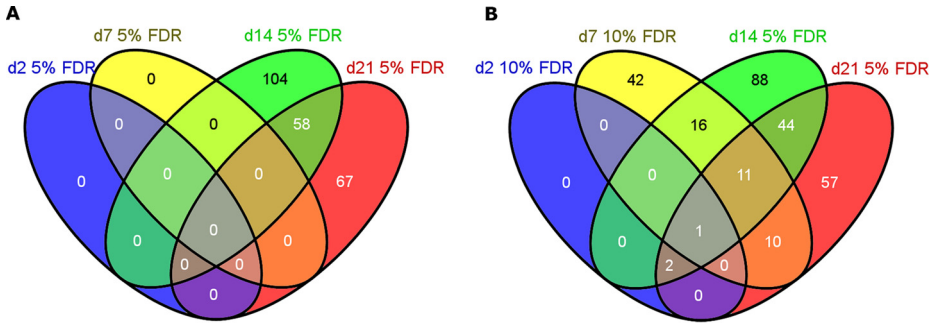

FIG. 1. **Safflower oil HFD induced hepatic insulin resistance is associated with differential protein expression.** Liver samples of mice fed HFD or LFD for the indicated 2, 7, 14, or 21d were compared by quantitative proteomics ($n = 6–8$) as described under "Experimental Procedures". Protein identification was performed using Mascot and proteins were subjected to label-free quantification in Progenesis LC-MS. Regulated proteins were identified using t-tests followed by Benjamini Hochberg correction. Cutoff values for regulation were: *a*, $q<0.05$ for all time points and (*b*) $q<0.05$ for d14 and d21, $q<0.1$ for d2 and d7. Venn diagrams show the overlap of regulated proteins at different time-points for different false discovery rates.

of overall proteome coverage, we therefore employed a membrane enrichment strategy without fractionation (14). We combined this approach with MS intensity based label-free quantification using Progenesis QI yielding an average coefficient of variation (CV) of 13% for the whole workflow including sample preparation (Supplement Table IV).

For each time point, individual mice ($n = 6–8$) were compared, yielding variable numbers of identified proteins (d2: 561, d7:555, d14:663, d21: 632). We identified 165 and 126 regulated proteins at d14 and d21, respectively, at 5% false discovery rate (FDR) (Fig. 1*a*). In order to identify regulated proteins at earlier time points it was necessary to adjust the FDR cutoff. For this reason 3 and 80 regulated proteins at 10% FDR were identified for and d2 and d7, respectively (Fig. 1*b*). We expected progressive down-regulation of hepatic insulin resistance associated proteins over the duration of the feeding experiment. Contrary to this expectation, the majority of regulated protein was found to be differentially expressed at one time point only. We proceeded to search for common patterns for the proteins found regulated at d14 and d21.

In order to identify underlying biochemical pathways we used pathway enrichment analysis against a customized liver proteome background set (constructed from (23) and proteins identified in this study) to distinguish diet- from liver-specific pathways. Identified enriched pathways for each time point are listed in Table I.

We found a set of metabolic pathways enriched at both d14 and d21. The general increase of enrichment factors from d14 to d21 implies that more components of the individual pathways were found regulated as hepatic insulin resistance progressed.

HFD Induced Hepatic Insulin Resistance is Associated with Deregulation of the EET Pathway—Upon closer examination, most pathways proved unlikely candidates for an association with hepatic insulin resistance, since they were either only transiently altered or reflected known metabolic adaptations occurring in response to high fat challenges.

Three candidate pathways, however, appeared potentially related to insulin resistance: the EET pathway, oxidative phosphorylation and retinol metabolism. Closer examination of regulated proteins on a pathway map of "Arachidonic acid metabolism" and "Linoleic acid metabolism" revealed that the EET pathway was the biological process affected by HFD feeding (Fig. S1). We chose the EET pathway over the other two candidates, because it is amenable to pharmacological manipulation and has already been implicated in signal transduction processes and glucose homeostasis.

The EET pathway consists of EET epoxygenases of the CYP2C and J families as well as the EET hydrolase Ephx2, which are responsible for the synthesis and degradation of EETs, respectively (3) (Fig. 2*c*). We found a progressive down-regulation of the EET epoxygenases beginning at d7 and statistically significant at d14 for CYP2C50, 67 and 70. At d21 all enzymes were significantly downregulated (Fig. 2*a*). In contrast, a more than 3-fold up-regulation of Ephx2, which degrades EETs to inactive dihydroxytrienoic acids (DHET), became statistically significant at d14 and d21 (Fig. 2*b*). In addition, we found a very similar pattern of down-regulation for CYP4A12 (Fig. 2*a*). This enzyme is involved in the ω-hydroxylation of EETs which is an intermediate step in the synthesis of 20-OH-DHETs (Fig. 2*c*). In contrast to unmodified DHETs, 20-OH-DHETs are biologically active as potent PPAR-α agonists (3). The down-regulation of CYP2C50, CYP2C70 and CYP2J5 as well as the up-regulation of Ephx2 were verified by a second independent method: SRM based absolute quantification of protein levels in crude liver protein extracts without membrane protein enrichment (Fig. 3). While the observed fold changes of these enzymes determined by SRM were closer to one, the temporal pattern of statistically significant expression changes could be confirmed for all four proteins (Fig. 3).

Ephx2 and the CYP enzymes are expressed in peroxisomes and ER, respectively. In order to exclude the possibility that the observed expression changes were the result of altera-

TABLE I

KEGG pathways underlying HFD induced differential protein expression. Numbers correspond to fold enrichment versus the background set. n.s. = not significant. Gene symbols of up- and down-regulated proteins are shown in bold and regular font, respectively. Regulated proteins for the data set with the highest enrichment factor are listed

KEGG pathway	Fold enrichment			Proteins
	d7	d14	d21	
Oxidative phosphorylation	n.s.	5.6	7.5	Atp5f1 Atp5l Cox5a Cox6a1 Cox6b Cyc1 Ndufa10 Ndufa5 Ndufa9 Ndufb7 Ndufb9 Ndufs1 Ndufs2 Ndufs5 Ndufs7 Sdha Sdhb Sdhc Uqcrb Uqcrc1 Uqcrh
Drug metabolism	n.s.	5.2	6.5	Cyp1a2 Cyp2a5 Cyp2a12 Cyp2c29 Cyp2c50 Cyp2c67 Cyp2c70 Cyp2e1 Cyp2f2 Ephx1 Fmo5 Gstp1 Maoa Ugt2b36 Ugt1a9
Arachidonic acid metabolism	n.s.	5.0	6.8	Cyp2c29 Cyp2c50 Cyp2c70 Cyp2c67 Cyp2e1 Cyp2j5 Cyp4a12 **Ephx2**
Linoleic acid metabolism	n.s.	n.s.	8.6	Cyp1a2 Cyp2c29 Cyp2c50 Cyp2c67 Cyp2c70 Cyp2e1Cyp2j5
Retinol metabolism	n.s.	4.8	6.5	Cyp1a2 Cyp2a5 Cyp2a12 Cyp2c29 Cyp2c50 Cyp2c67 Cyp2c70 Cyp4a12 Ugt1a9 Ugt2b36
Primary bile acid biosynthesis	n.s.	7.2	n.s.	**Baat** Cyp27a1 Cyp7a1**Hsd17b4 Scp2**
Biosynthesis of unsaturated fatty acids	n.s.	7.2	n.s.	**Acaa1a Acaa1b Acox1 Baat Hadha**
PPAR signaling pathway	n.s.	3.7	n.s.	**Acaa1a Acaa1b Acox1 Apoa1** Cyp27a1 Cyp7a1 Cyp4a12 **Scp2**
Steroid hormone biosynthesis	n.s.	n.s.	7.3	Cyp7a1 Cyp7b1 Comt1 Hsd3b5 Hsd17b2 Ugt1a9 Ugt2b36
Cardiac muscle contraction	n.s.	n.s.	5.3	Cox6a1 Cox6b1 Cyc1 Cox5a Uqcrb Uqcrc1 Uqcrh
Ribosome	7.7	n.s.	n.s.	**Rpl13 Rpl32 Rpl19 Rpl12 Rps11 Rps27a Rps16 Rps2 Rps14 Rps26 Rps15a Rps3 Rps8**

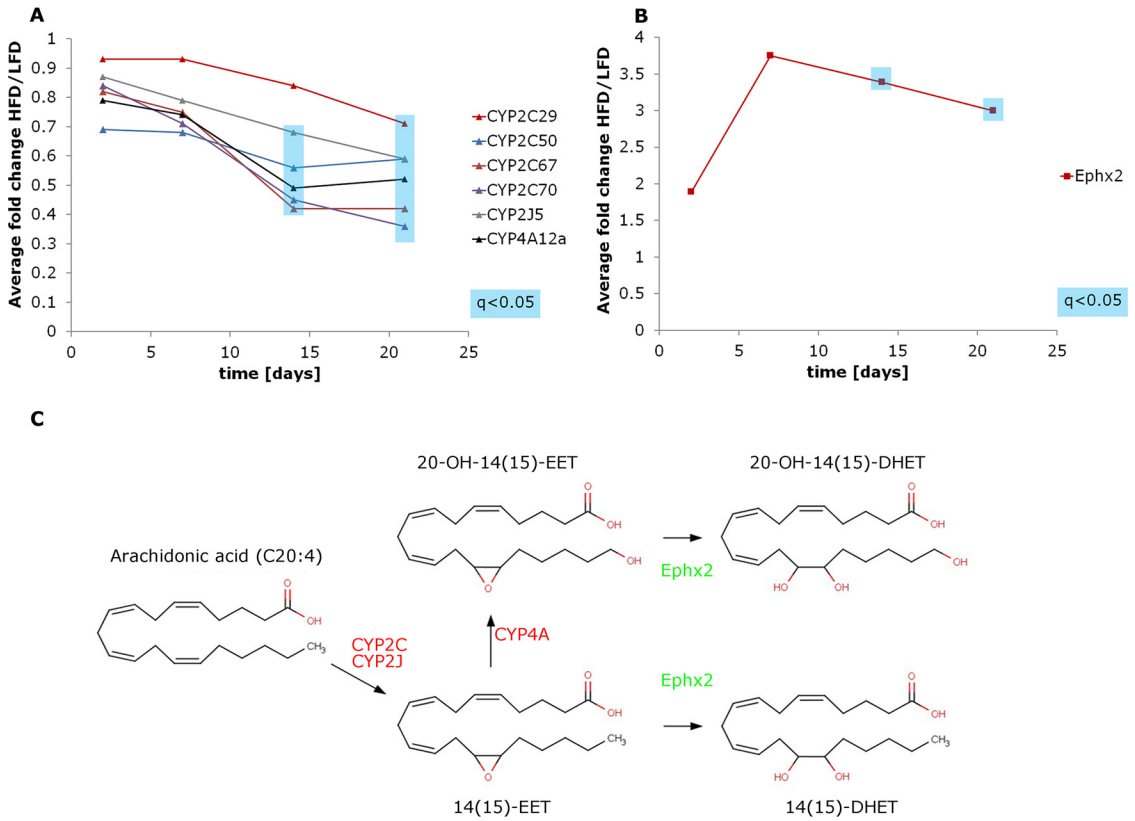

FIG. 2. **EET pathway enzymes are deregulated through safflower oil HFD feeding at d14 and d21.** Quantification of EET enzymes in mouse liver based on non-targeted proteomics data (*a*, *b*). Time course of average fold changes of EET synthesizing CYP enzymes (*a*) and Ephx2 (*b*). Statistical significance at 5% FDR is shown through blue shading. (c) EET synthesis and degradation pathway. Up- and downregulated enzymes are shown in green and red, respectively.

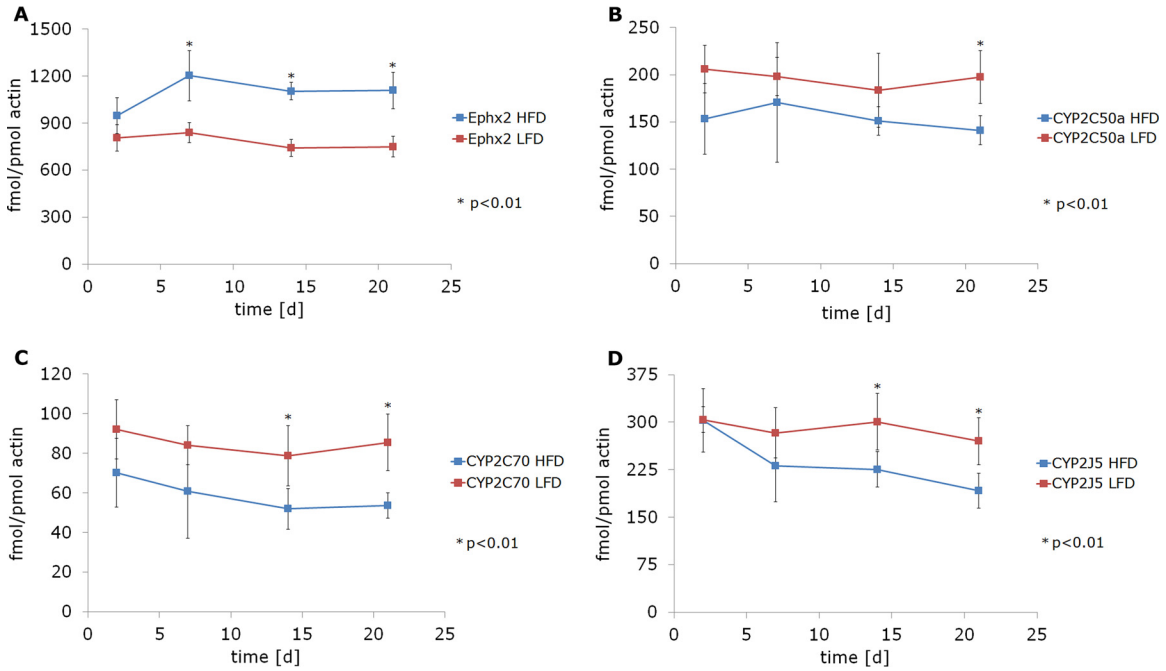

FIG. 3. **Validation of differential EET pathway enzyme expression in crude liver protein extracts by LC-SRM.** For each sample, ten μg protein from crude liver extracts were digested with trypsin overnight and heavy labeled internal standard peptides were added. Absolute amounts of Ephx2 (*a*), CYP2C50a (*b*), CYP2C70 (*c*), and CYP2J5 (*d*) normalized to $\beta\gamma$-actin were determined by the LC-SRM method described under "Experimental Procedures" and Supplement Table III. Values represent mean ± S.D. for seven mice at each time point in each group.

TABLE II

*Repression of EET synthesizing CYPs is not a consequence of changes in ER abundance or general CYP repression. Relative quantifications for the indicated proteins were extracted from nontargeted proteomics datasets. Average fold changes ($n = 6–8$) are given for each protein and time point. Significance level: * $p < 0.01$*

Protein	Average fold change HFD/LFD			
	d2	d7	d14	d21
Calnexin	1.07	0.89	0.75	0.81
Catalase	1.12	1.47	0.43	0.95
CYP3A11	0.95	0.95	1.02	0.78
CYP2C70	0.84	0.71	0.45*	0.36*

tions in subcellular structure, we compared the abundance of markers for both organelles. We found no differences in the abundance of either the ER marker calnexin or the peroxisome marker catalase at any time point (Table II). Moreover, the up-regulation of Ephx2 (1.25fold by d21) and down-regulation of CYP2C70 (0.6fold by d21) and CYP2C67 (0.7fold by d21) was also observed at the transcript level, although this was not the case for the four other CYPs (24).

In total we quantified 31 CYP enzymes in this study. Of these, 17 were not affected by safflower oil HFD feeding. As an example we compared the expression of CYP2C70 and CYP3A11, a homologue of the human CYP3A4, whose expression can be induced by a large number of xenobiotics (25). The expression of CYP3A11 was very stable across time points, while there was a clear down-regulation for CYP2C70 at d14 and d21 (Table II). Of the 14 CYPs affected by safflower oil HFD feeding, 13 were associated with the enriched pathways and six of them were part of the EET pathway (Fig. 2*c*). We conclude that CYP repression was not exclusive to EET epoxygenases. However, the affected CYPs were components of distinct HFD sensitive biochemical pathways and the EET pathway was most prominently affected among these pathways.

EETs Pathway Enzymes have No Impact on Insulin Signaling in Absence of Arachidonic Acid—As the results implicating EETs were based on observations of altered EET pathway enzyme expression levels, we next investigated whether these enzymes themselves had an impact on insulin signaling. Ephx2 in particular could influence the phosphorylation cascade in cells as it has phosphatase as well as epoxide hydrolase activity (26).

In order to test possible effect of the EET pathway enzymes on insulin signaling, we analyzed the effect of EET enzyme overexpression on the insulin signaling cascade in cell culture. As readout we assessed phosphorylation of the three key nodes IR (three tyrosine motif), IRS-1 (Y608) and Akt (S473) (27). We used 1.5 nM insulin, resembling high physiological concentrations, which can occur in the portal vein (28), as well as a supraphysiological dose of 100 nM insulin. Based on preliminary experiments we chose 40 min and 60 min to ensure activation of all three signaling proteins (Fig. S2).

In order to study EET independent effect we used an EET and arachidonic acid free cell system that allowed overex-

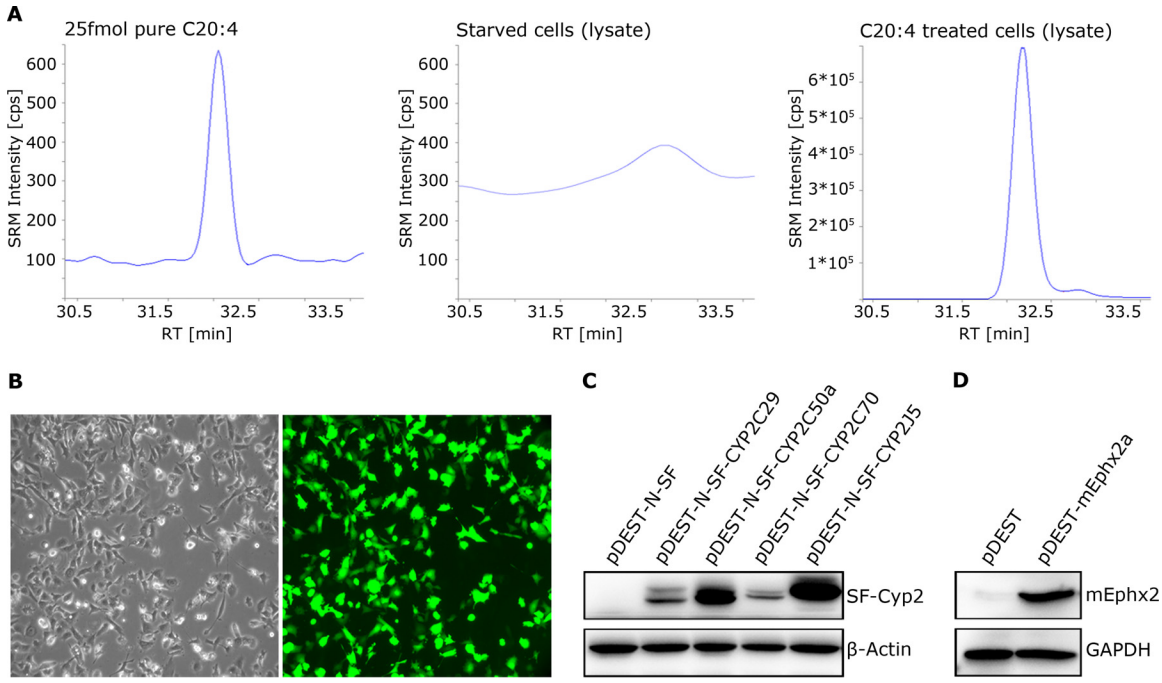

FIG. 4. **The influence of EET enzyme overexpression on insulin signaling was studied in Hepa 1–6 cells in absence of free arachidonic acid.** *a*, Measurement of arachidonic acid (C20:4) content in Hepa 1–6 cells by LC-SRM. From left to right: 25fmol pure arachidonic acid, lipid extract of serum starved Hepa 1–6 cells, lipid extract of starved Hepa 1–6 cells treated with 150 μM free arachidonic acid for 1h. *b*, Transfection efficiency. Hepa 1–6 cell were transfected using Lipofektamine 2000 with the reporter plasmid pCMV-GFP. Phase contrast (left) and direct fluorescence (right) pictures were taken 24 h after transfection using an epifluorescence live cell microscope. *c*, Hepa 1–6 cells were transfected with empty vector or constructs encoding N-terminal strep-flag (SF) tagged CYP enzymes. Cells were lysed after 24 h and SF constructs detected by Western blot using an anti-Flag antibody. *d*, Hepa 1–6 cells were transfected with empty vector or the mEphx2a construct, harvested after 24 h and Ephx2 was detected by Western blot with an Ephx2 specific antibody.

pression of EET pathway enzymes. When cells were serum starved overnight, we were unable to detect arachidonic acid by LC-MS in their lysates (Fig. 4*a*, middle panel). For comparison 25fmol pure arachidonic acid gave a clear signal in this assay (Fig. 4*a*, left panel). When free arachidonic acid was added to the medium of starved cells it could readily be detected again in lysates (Fig. 4*a*, right panel). In addition, no EETs or DHETs were detectable in lysates of starved cells, although the limit of detection for our assay was in the nM range. Hepa 1–6 cells could be transfected with high efficiency (Fig. 4*b*) and the EET enzymes encoded in the expression constructs were readily detectable by immunoblot (Fig. 4*c*, *d*).

We proceeded to conduct insulin stimulation of transfected, serum starved cells. When comparing IRS-1, IR or Akt phosphorylation with or without insulin at different time points, we found no impact of any of the five EET enzymes tested in comparison to empty vector transfected cells (Fig. 5).

We conclude that even with exhaustive measures taken, no impact of the EET enzymes Ephx2, CYP2C29, CYP2C50a, CYP2C70 or CYP2J5 on insulin signaling could be observed.

EETs Enhance Insulin Induced Akt Activation in Primary Hepatocytes without Affecting IR or IRS-1 Phosphorylation—Finally, we tested the effects of exogenous EETs on insulin signaling in primary hepatocytes from normal diet-fed C3HeB/FeJ mice. Primary hepatocytes were treated with 1.5 nM and 100 nM insulin with or without 4 μM of each EET isomer. As the concentration of all EET isomers in mouse liver were determined to be ~0.4–1 μM (29), these concentrations are likely not far from the physiological range in mice. As there is evidence for an intracellular mechanism of EET action we included pre-treatment of cells with EETs for 1h to allow the eicosanoids to accumulate in the cells before the start of the insulin/EET costimulation.

We found that EET treatment alone indeed induced Akt S473 phosphorylation after both, 40 min and 60 min costimulation (Fig. 6). The addition of 4 μM EETs to 1.5 nM insulin increased Akt phosphorylation almost to the level found for 100 nM insulin at both 40 min and 60 min. Pre-treatment was necessary to elicit this effect for 40 min but not for 60 min costimulation (Fig. 6).

In contrast, we found no effect of EETs on insulin mediated IR activation at any concentration or time point (Fig. 6). However, we noted a small increase in phospho IRS-1 at 1.5 nM insulin though EETs (Fig. 6), though this effect could not be reproduced in replicate experiments. EETs had no effect on IRS-1 phosphorylation at 100 nM insulin (Fig. 6). No changes in the expression of IRS-1, IR or Akt were evident (Fig. 6).

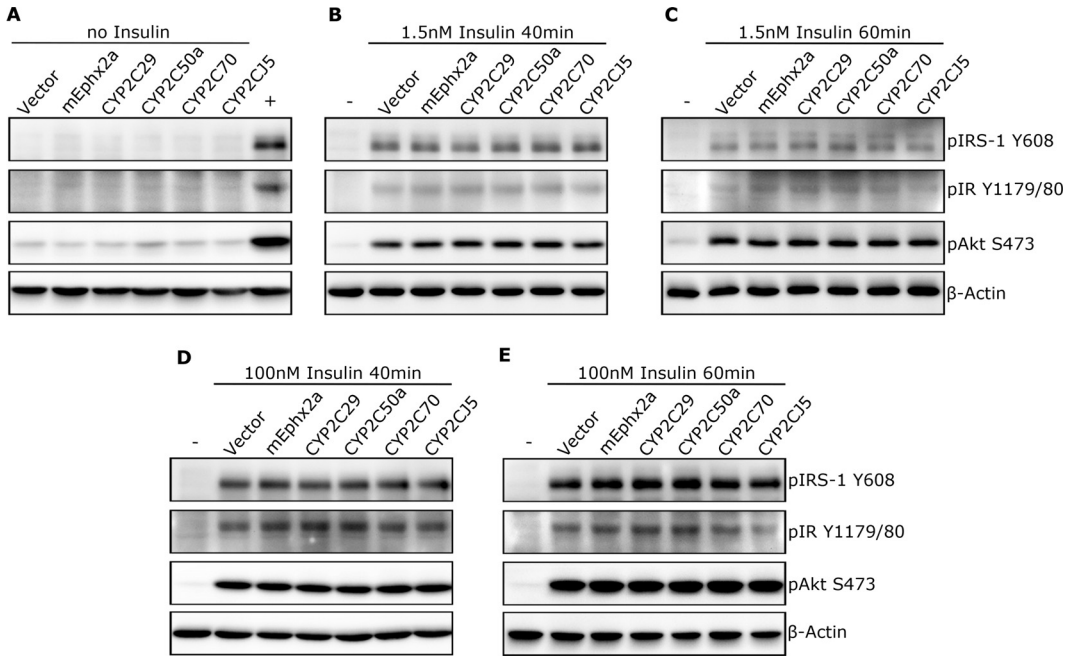

FIG. 5. **EET enzyme overexpression in absence of arachidonic acid does not influence insulin signaling.** Hepa 1–6 were transfected with the empty vector or the indicated constructs, serum starved and stimulated with insulin 24h after transfection. Phosphorylation of pIRS-1, pIR and pAkt were determined under basal conditions (*a*), at 1.5 nM insulin after 40 min (*b*), and 60 min (*c*) as well as at 100 nM insulin after 40 min (*d*) and 60 min (*e*). Ten μg protein for each condition were separated by SDS-PAGE on 10% gels, blotted onto PVDF membranes and target proteins were visualized by immunodetection. Untransfected Hepa 1–6 cells, mock-stimulated or stimulated with 100 nM insulin, served as negative control (-) and positive control, (+) respectively. Total IR, IRS-1 and Akt levels were not affected by insulin stimulation of transfected cell (supplemental Fig. S3). Apparent MWs were: phospho-IRS-1 (pIRS-1): ~200kDa, phospho-IR (pIR): ~100 kDa, phospho Akt (pAkt): ~55 kDa, β-Actin ~40 kDa. Representative example of three experiments.

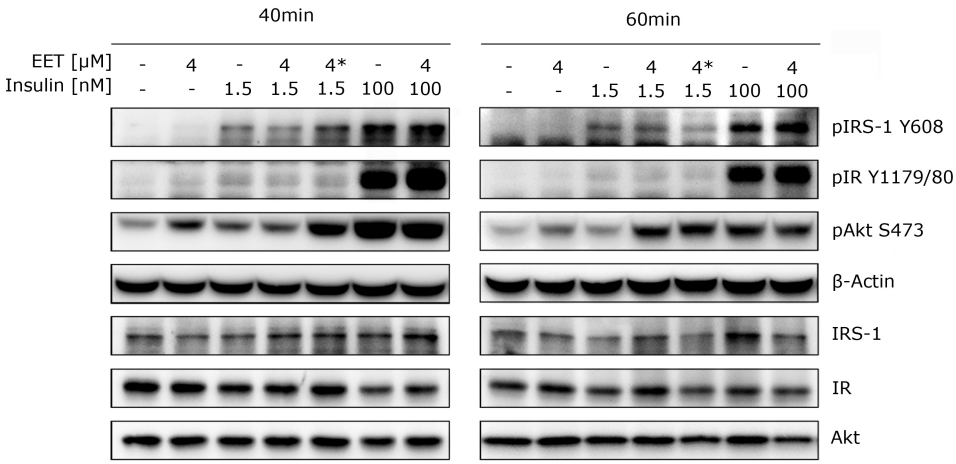

FIG. 6. **EETs enhance Akt activation through insulin in primary mouse hepatocytes.** Primary hepatocytes were starved of serum overnight and stimulated with insulin and/or 4 μM of each EET isomer. Asterisk (*) denoted cells pre-treated with 4 μM EETs for 1h before the start of insulin stimulation. Irrespective of EET treatment, all wells contained DMSO at the same final concentration. Ten μg protein for each condition were separated by SDS-PAGE on 10% gels, blotted onto PVDF membranes and target proteins were visualized by immunodetection. Apparent MWs were: pIRS-1/IRS-1: ~200kDa, pIR/IR: ~100 kDa, pAkt/Akt: ~55 kDa, β-Actin ~40 kDa. Representative example of two experiments. Quantification of Western blot data is provided in supplemental Fig. S3.

Quantification of Western blot data and normalization of phosphoprotein derived signals to total protein levels confirmed the observation stated above (Fig. S4).

We confirmed the robust EET mediated increase in Akt phosphorylation at 1.5 nM insulin without changes in IR or IRS-1 phosphorylation in the hepatocyte cell lines BNL CL.2 (Fig. S5) and Hepa 1–6 (data not shown). Based on these results we conclude that EETs are indeed positive modifiers of insulin signaling in hepatocytes, taking effect at the level of Akt. It is important to note that the data presented here only

support a role of EETs as modifiers of insulin signaling. Conclusions whether this effect is additive or synergistic and if EETs may be classified as insulin sensitizers are too far reaching based on the presented data.

DISCUSSION

In this study, we could demonstrate that EETs influence insulin signaling and are affected by dietary conditions promoting hepatosteatosis and hepatic insulin resistance. Furthermore, we show that the impact of the EET pathway on insulin signaling is conferred by the eicosanoids which implies that the role of the EET enzymes lies in regulating the levels of the eicosanoids through their activity. In light of the positive influence of EETs on insulin signaling, down-regulation of the pathway in insulin resistant liver appears to be an alteration contributing to hepatic insulin resistance rather than a defense mechanism against it.

The first evidence implicating EETs in metabolic disorders was reported more than 25 years ago by Thomas *et al.*, who showed that cytoplasmic epoxide hydrolase activity was impacted by experimental diabetes and re-feeding of rats (30). Intriguingly, an unrelated study found that EET mediated relaxation of mesenteric arteries was completely lost in HFD-fed insulin resistant rats (31). Recently, four different studies have shown different beneficial effects of the EET pathway in rodent models of type 2 diabetes. Glucose tolerance could be improved through Ephx2 knockout in mice (10, 11) as well as EET epoxygenase overexpression in rats (12). As none of these models included organ specific manipulation of the EET pathway and EETs were found to increase insulin secretion (10, 11) as well as pancreatic islet size (11), there is currently conflicting evidence concerning the influence of EETs on insulin sensitivity. Luo *et al.* concluded that EETs do not influence insulin sensitivity since they found no difference in insulin tolerance tests when comparing Ephx2$^{-/-}$ mice to controls (10). In contrast, Luria *et al.* showed increased IR, IRS-1 and Akt phosphorylation in livers of Ephx2$^{-/-}$ mice, but this finding was confounded by elevated insulin levels in these mice (11). Hence it was not possible to separate the effect of higher levels of insulin and putative changes in liver EET concentrations on hepatic insulin signaling in this particular study.

In contrast to hepatocytes, the autocrine signaling function of EETs in endothelial cells has been studied extensively. EETs have been shown to activate Akt (4, 5) as well as the MAP kinase p42/44 ERK (6) and inhibit FOXO1 and FOXO3 (4). Interestingly, these signaling molecules are affected by insulin in hepatocytes in the same way (27). On the other hand, EETs have been shown to increase cAMP levels and activate PKA in endothelial cells (32). In this regard EETs would behave like antagonists of insulin signaling (*e.g.* glucagon).

The mechanism behind the influence of EETs on intracellular signaling is not known. The current opinion is that they bind to a receptor, but it is unclear whether this putative receptor is a transmembrane protein, reacting to extracellular ligands, or an intracellular receptor (3). Our results imply that EETs converge on insulin signaling at the level of Akt but exert their effect though a parallel pathway intersecting with the insulin signaling pathway downstream of IRS-1. It has already been shown that activation of Akt in HepG2 cells through EETs could be blocked by inhibiting PI3K (13). Assuming that the same mechanism underlies EET mediated Akt activation in both cell types, our data supports a model in which EETs intersect with insulin signaling downstream of IRS-1 and upstream of PI3K. By the same token, the data presented here are not in accord with activation of the insulin signaling pathway through EETs upstream of the IR (11).

Genetic evidence supports a role of EETs in insulin sensitivity in humans. Japanese patients bearing the Ephx2 Arg287Glu mutation had lower insulin sensitivity as determined by euglycemic-hyperinsulinemic clamps (33). The same mutation was also found to lower plasma triglycerides and cholesterol levels in patients with familial hypercholesterolemia (34).

The fact that Ephx2 inhibitors are currently under investigation in clinical trials opens the possibility to investigate their value for the treatment of insulin resistance. While Ephx2 inhibitor treatment failed to improve glucose tolerance in one study (11), an improvement of glucose tolerance was shown in a second study after 16 weeks treatment of rats on HFD with a different Ephx2 inhibitor. In these rats, Ephx2 inhibition also lowered blood pressure and reduced plasma free fatty acids but increased plasma triglycerides (35).

It is tempting to speculate that the expression changes in the liver upon HFD feeding are related to the influence of polyunsaturated fatty acids on transcription. One of the most prominent roles of these types of fatty acids is regulation of the transcription factors PPAR-α (36). Furthermore, PPAR-α has been found to induce and repress Ephx2 and CYP2C isoform expression, respectively (37, 38). Our pathway enrichment analysis and transcriptome analysis of the safflower oil HFD model confirmed PPAR-α activation: 37, 107, 82 and 67 PPAR target genes were found activated at d2, d7, d14 and d21, respectively (24).

The extensive role of EETs in blood vessels raises the question whether hepatocytes are the cell type affected in the safflower oil HFD model. This seems likely as histochemical expression analysis of a human tissue microarray has shown that hepatocytes are the main cells expressing Ephx2, CYP2C isoform and CYP2J2 (ortholog of CYP2J5) in liver tissue (39).

CONCLUSION

The EET pathway has become a promising new player in the pathophysiology of insulin resistance. It clearly influences insulin secretion and very likely modifies insulin sensitivity. Here we have shown that the EET pathway is regulated by HFD feeding and can modulate insulin signaling in hepatocytes. Future studies in mouse models will help determine the

functional impact of the EET pathway on hepatic insulin sensitivity and may substantiate its value as a target for the treatment of hepatic insulin resistance.

Acknowledgments—We thank Sandra Helm and Silke Becker for excellent technical support with the LC-MS systems as well as Dr. Lorenza D'Alessandro and Prof. Ursula Klingmüller for sharing their expertise on primary hepatocytes. We would also like to thank Connie Cepko (Howard Hughes Medical Institute, Harvard College) for sharing the pCMV-GFP construct via Addgene. We declare no conflict of interest.

* This work was supported by grants from the German Federal Ministry of Education and Research (BMBF): Grant number 03IS2061B GANI_MED (Greifswald Approach to Individualized Medicine) and a second grant to the German Center for Diabetes Research (DZD e.V.).

[S] This article contains supplemental Figs. S1 to S5 and Tables S1 to S4.

§§ To whom correspondence should be addressed: Hauck, Research Unit Protein Science, Helmholtz Center Munich, German Research Center for Environmental Health (GmbH), Ingolstädter Landstr. 1, 85764 Neuherberg. Tel.: 0049-89-3187-394; E-mail: hauck@helmholtz-muenchen.de.

REFERENCES

1. DeFronzo, R. A. (2004) Pathogenesis of type 2 diabetes mellitus. *Med. Clin. North Am.* **88,** 787–835, ix
2. DeFronzo, R. A., Ferrannini, E., and Simonson, D. C. (1989) Fasting hyperglycemia in non-insulin-dependent diabetes mellitus: contributions of excessive hepatic glucose production and impaired tissue glucose uptake. *Metabolism* **38,** 387–395
3. Spector, A. A., and Norris, A. W. (2007) Action of epoxyeicosatrienoic acids on cellular function. *Am. J. Physiol. Cell Physiol.* **292,** C996–C1012
4. Potente, M., Fisslthaler, B., Busse, R., and Fleming, I. (2003) 11, 12-Epoxyeicosatrienoic acid-induced inhibition of FOXO factors promotes endothelial proliferation by down-regulating p27Kip1. *J. Biol. Chem.* **278,** 29619–29625
5. Pozzi, A., Macias-Perez, I., Abair, T., Wei, S., Su, Y., Zent, R., Falck, J. R., and Capdevila, J. H. (2005) Characterization of 5, 6-and 8, 9-epoxyeicosatrienoic acids (5, 6-and 8, 9-EET) as potent in vivo angiogenic lipids. *J. Biol. Chem.* **280,** 27138–27146
6. Wang, Y., Wei, X., Xiao, X., Hui, R., Card, J. W., Carey, M. A., Wang, D. W., and Zeldin, D. C. (2005) Arachidonic acid epoxygenase metabolites stimulate endothelial cell growth and angiogenesis via mitogen-activated protein kinase and phosphatidylinositol 3-kinase/Akt signaling pathways. *J. Pharmacol. Exp. Ther.* **314,** 522–532
7. Campbell, W. B., Gebremedhin, D., Pratt, P. F., and Harder, D. R. (1996) Identification of epoxyeicosatrienoic acids as endothelium-derived hyperpolarizing factors. *Circ. Res.* **78,** 415–423
8. Node, K., Huo, Y., Ruan, X., Yang, B., Spiecker, M., Ley, K., Zeldin, D. C., and Liao, J. K. (1999) Anti-inflammatory properties of cytochrome P450 epoxygenase-derived eicosanoids. *Science* **285,** 1276–1279
9. Imig, J. D., and Hammock, B. D. (2009) Soluble epoxide hydrolase as a therapeutic target for cardiovascular diseases. *Nat. Rev. Drug Discov.* **8,** 794–805
10. Luo, P., Chang, H.-H., Zhou, Y., Zhang, S., Hwang, S. H., Morisseau, C., Wang, C.-Y., Inscho, E. W., Hammock, B. D., and Wang, M.-H. (2010) Inhibition or deletion of soluble epoxide hydrolase prevents hyperglycemia, promotes insulin secretion, and reduces islet apoptosis. *J. Pharmacol. Exp. Ther.* **334,** 430–438
11. Luria, A., Bettaieb, A., Xi, Y., Shieh, G.-J., Liu, H.-C., Inoue, H., Tsai, H.-J., Imig, J. D., Haj, F. G., and Hammock, B. D. (2011) Soluble epoxide hydrolase deficiency alters pancreatic islet size and improves glucose homeostasis in a model of insulin resistance. *Proc. Natl. Acad. Sci. U.S.A.* **108,** 9038–9043
12. Xu, X., Zhao, C. X., Wang, L., Tu, L., Fang, X., Zheng, C., Edin, M. L., Zeldin, D. C., and Wang, D. W. (2010) Increased CYP2J3 expression reduces insulin resistance in fructose-treated rats and db/db mice. *Diabetes* **59,** 997–1005
13. Skepner, J. E., Shelly, L. D., Ji, C., Reidich, B., and Luo, Y. (2011) Chronic treatment with epoxyeicosatrienoic acids modulates insulin signaling and prevents insulin resistance in hepatocytes. *Prostaglandins Other Lipid Mediat.* **94,** 3–8
14. Hauck, S. M., Dietter, J., Kramer, R. L., Hofmaier, F., Zipplies, J. K., Amann, B., Feuchtinger, A., Deeg, C. A., and Ueffing, M. (2010) Deciphering membrane-associated molecular processes in target tissue of autoimmune uveitis by label-free quantitative mass spectrometry. *Mol. Cell. Proteomics* **9,** 2292–2305
15. Kall, L., Storey, J. D., MacCoss, M. J., and Noble, W. S. (2008) Posterior error probabilities and false discovery rates: two sides of the same coin. *J. Proteome Res.* **7,** 40–44
16. Schäfer, A., von Toerne, C., Becker, S., Sarioglu, H., Neschen, S., Kahle, M., Hauck, S. M., and Ueffing, M. (2012) Two-Dimensional Peptide Separation Improving Sensitivity of Selected Reaction Monitoring-Based Quantitative Proteomics in Mouse Liver Tissue: Comparing Off-Gel Electrophoresis and Strong Cation Exchange Chromatography. *Anal. Chem.* **84,** 8853–8862
17. Lange, V., Picotti, P., Domon, B., and Aebersold, R. (2008) Selected reaction monitoring for quantitative proteomics: a tutorial. *Mol. Syst. Biol.* **4,** 222
18. Klingmuller, U., Bauer, A., Bohl, S., Nickel, P. J., Breitkopf, K., Dooley, S., Zellmer, S., Kern, C., Merfort, I., Sparna, T., Donauer, J., Walz, G., Geyer, M., Kreutz, C., Hermes, M., Gotschel, F., Hecht, A., Walter, D., Egger, L., Neubert, K., Borner, C., Brulport, M., Schormann, W., Sauer, C., Baumann, F., Preiss, R., MacNelly, S., Godoy, P., Wiercinska, E., Ciuclan, L., Edelmann, J., Zeilinger, K., Heinrich, M., Zanger, U. M., Gebhardt, R., Maiwald, T., Heinrich, R., Timmer, J., von Weizsacker, F., and Hengstler, J. G. (2006) Primary mouse hepatocytes for systems biology approaches: a standardized in vitro system for modelling of signal transduction pathways. *IEE Proc. Syst. Biol.* **153,** 433
19. Chomczynski, P., and Sacchi, N. (1987) Single-step method of RNA isolation by acid guanidinium thiocyanate-phenol-chloroform extraction. *Anal. Biochem.* **162,** 156–159
20. Gloeckner, C. J., Boldt, K., Schumacher, A., Roepman, R., and Ueffing, M. (2007) A novel tandem affinity purification strategy for the efficient isolation and characterisation of native protein complexes. *Proteomics* **7,** 4228–4234
21. Da Wei Huang, B. T. S., and Lempicki, R. A. (2008) Systematic and integrative analysis of large gene lists using DAVID bioinformatics resources. *Nat. Protoc.* **4,** 44–57
22. Kahle, M., Schäfer, A., Seelig, A., Schultheiβ, J., Wu, M., Aichler, M., Leonhardt, J., Rathkolb, B., Rozman, J., Sarioglu, H., Hauck, S. M., Ueffing, M., Wolf, E., Kastenmueller, G., Adamski, J., Walch, A., Hrabé de Angelis, M., and Neschen, S. (2015) High fat diet-induced modifications in membrane lipid and mitochondrial-membrane protein signatures precede the development of hepatic insulin resistance in mice. *Mol. Metab.* **4,** 39–50
23. Lai, K. K., Kolippakkam, D., and Beretta, L. (2008) Comprehensive and quantitative proteome profiling of the mouse liver and plasma. *Hepatology* **47,** 1043–1051
24. Kahle, M., Horsch, M., Fridrich, B., Seelig, A., Schultheiss, J., Leonhardt, J., Irmler, M., Beckers, J., Rathkolb, B., Wolf, E., Franke, N., Gailus-Durner, V., Fuchs, H., de Angelis, M. H., and Neschen, S. (2013) Phenotypic comparison of common mouse strains developing high-fat diet-induced hepatosteatosis. *Mol. Metab.* **2,** 435–446
25. Martinez-Jimenez, C. P., Jover, R., Donato, M. T., Castell, J. V., and Gomez-Lechon, M. J. (2007) Transcriptional regulation and expression of CYP3A4 in hepatocytes. *Curr. Drug Metab.* **8,** 185–194
26. Newman, J. W., Morisseau, C., Harris, T. R., and Hammock, B. D. (2003) The soluble epoxide hydrolase encoded by EPXH2 is a bifunctional enzyme with novel lipid phosphate phosphatase activity. *Proc. Natl. Acad. Sci. U.S.A.* **100,** 1558–1563
27. Taniguchi, C. M., Emanuelli, B., and Kahn, C. R. (2006) Critical nodes in signalling pathways: insights into insulin action. *Nat. Rev. Mol. Cell Biol.* **7,** 85–96
28. Song, S. H., McIntyre, S. S., Shah, H., Veldhuis, J. D., Hayes, P. C., and Butler, P. C. (2000) Direct measurement of pulsatile insulin secretion from the portal vein in human subjects. *J. Clin. Endocrinol. Metab.* **85,**

4491–4499
29. Arnold, C., Markovic, M., Blossey, K., Wallukat, G., Fischer, R., Dechend, R., Konkel, A., von Schacky, C., Luft, F. C., and Muller, D. N. (2010) Arachidonic acid-metabolizing cytochrome P450 enzymes are targets of ω-3 fatty acids. *J. Biol. Chem.* **285,** 32720–32733
30. Thomas, H., Schladt, L., Knehr, M., and Oesch, F. (1989) Effect of diabetes and starvation on the activity of rat liver epoxide hydrolases, glutathione S-transferases and peroxisomal β-oxidation. *Biochem. Pharmacol.* **38,** 4291–4297
31. Miller, A. W., Dimitropoulou, C., Han, G., White, R. E., Busija, D. W., and Carrier, G. O. (2001) Epoxyeicosatrienoic acid-induced relaxation is impaired in insulin resistance. *Am. J. Physiol. Heart Circ. Physiol.* **281,** H1524–H1531
32. Node, K., Ruan, X. L., Dai, J., Yang, S. X., Graham, L., Zeldin, D. C., and Liao, J. K. (2001) Activation of Galpha s mediates induction of tissue-type plasminogen activator gene transcription by epoxyeicosatrienoic acids. *J. Biol. Chem.* **276,** 15983–15989
33. Ohtoshi, K., Kaneto, H., Node, K., Nakamura, Y., Shiraiwa, T., Matsuhisa, M., and Yamasaki, Y. (2005) Association of soluble epoxide hydrolase gene polymorphism with insulin resistance in type 2 diabetic patients. *Biochem. Biophys. Res. Commun.* **331,** 347–350
34. Sato, K., Emi, M., Ezura, Y., Fujita, Y., Takada, D., Ishigami, T., Umemura, S., Xin, Y., Wu, L. L., Larrinaga-Shum, S., Stephenson, S. H., Hunt, S. C., and Hopkins, P. N. (2004) Soluble epoxide hydrolase variant (Glu287Arg) modifies plasma total cholesterol and triglyceride phenotype in familial hypercholesterolemia: intrafamilial association study in an eight-generation hyperlipidemic kindred. *J. Hum. Genet.* **49,** 29–34
35. Iyer, A., Kauter, K., Alam, M. A., Hwang, S. H., Morisseau, C., Hammock, B. D., and Brown, L. (2012) Pharmacological inhibition of soluble epoxide hydrolase ameliorates diet-induced metabolic syndrome in rats. *Exp. Diab. Res.* **2012,** 758614
36. Clarke, S. D. (2001) Polyunsaturated fatty acid regulation of gene transcription: a molecular mechanism to improve the metabolic syndrome. *J. Nutr.* **131,** 1129–1132
37. Newman, J. W., Morisseau, C., and Hammock, B. D. (2005) Epoxide hydrolases: their roles and interactions with lipid metabolism. *Prog. Lipid Res.* **44,** 1–51
38. Ripp, S. L., Falkner, K. C., Pendleton, M. L., Tamasi, V., and Prough, R. A. (2003) Regulation of CYP2C11 by dehydroepiandrosterone and peroxisome proliferators: identification of the negative regulatory region of the gene. *Mol. Pharmacol.* **64,** 113–122
39. Enayetallah, A. E., French, R. A., Thibodeau, M. S., and Grant, D. F. (2004) Distribution of soluble epoxide hydrolase and of cytochrome P450 2C8, 2C9, and 2J2 in human tissues. *J. Histochem. Cytochem.* **52,** 447–454